


CLINICAL TRIAL

Post COVID-19 syndrome with impairment of flow-mediated epicardial vasodilation and flow reserve

Amanda Verma^{1,2} | Tarun Ramayya² | Anand Upadhyaya¹ | Ines Valenta¹ |
Maureen Lyons³ | Jonas Marschall³ | Farrokh Dehdashti¹ | Robert J. Gropler¹ |
Pamela K. Woodard¹ | Thomas Hellmut Schindler^{1,2} 

¹Division of Nuclear Medicine, Mallinckrodt Institute of Radiology, Washington University School of Medicine, St. Louis, Missouri, USA

²Cardiovascular Division, John T. Milliken Department of Internal Medicine, Washington University School of Medicine, St. Louis, Missouri, USA

³Infectious Disease Division, John T. Milliken Department of Internal Medicine, Washington University School of Medicine, St. Louis, Missouri, USA

Correspondence

Thomas Hellmut Schindler, Washington University in St. Louis, Mallinckrodt Institute of Radiology-Division of Nuclear Medicine, 510 S. Kingshighway, Campus Box 8223, St. Louis, MO 63110, USA.
Email: thschindler@wustl.edu

Funding information

Washington University in St. Louis, Grant/Award Number: 12-3271- 93128

Abstract

Aims: The aim of this study is to evaluate whether post-acute sequelae of COVID-19 cardiovascular syndrome (PASC-CVS) is associated with alterations in coronary circulatory function.

Materials and Methods: In individuals with PASC-CVS but without known cardiovascular risk factors ($n = 23$) and in healthy controls (CON, $n = 23$), myocardial blood flow (MBF) was assessed with ¹³N-ammonia and PET/CT in mL/g/min during regadenoson-stimulated hyperemia, at rest, and the global myocardial flow reserve (MFR) was calculated. MBF was also measured in the mid and mid-distal myocardium of the left ventricle (LV). The Δ longitudinal MBF gradient (hyperemia minus rest) as a reflection of an impairment of flow-mediated epicardial vasodilation, was calculated.

Results: Resting MBF was significantly higher in PASC-CVS than in CON (1.29 ± 0.27 vs. 1.08 ± 0.20 ml/g/min, $p \leq .024$), while hyperemic MBFs did not differ significantly among groups (2.46 ± 0.53 and 2.40 ± 0.34 ml/g/min, $p = .621$). The MFR was significantly less in PASC-CVS than in CON (1.97 ± 0.54 vs. 2.27 ± 0.43 , $p \leq .031$). In addition, there was a Δ longitudinal MBF gradient in PASC-CVS, not observed in CON (-0.17 ± 0.18 vs. 0.04 ± 0.11 ml/g/min, $p < .0001$).

Conclusions: Post-acute sequelae of COVID-19 cardiovascular syndrome may be associated with an impairment of flow-mediated epicardial vasodilation, while reductions in coronary vasodilator capacity appear predominantly related to increases in resting flow in women deserving further investigations.

KEYWORDS

blood flow, CAD, circulation, coronary endothelial function, flow gradient, MFR, microvascular function, myocardial perfusion, PET

1 | INTRODUCTION

A new single-stranded RNA virus, named severe acute respiratory syndrome coronavirus 2 (SARS-CoV-2), was detected in December 2019, which can manifest as coronavirus disease 2019 (COVID-19) spanning a wide range of clinical scenarios.¹ In the worst-case scenario, COVID-19 may lead to severe pneumonia, which then rapidly advance to an acute respiratory distress syndrome and multiple organ failure.^{2–4} COVID-19 may also trigger cardiovascular complications associated with high morbidity and mortality.³ Convalescent patients, however, may suffer from cardiovascular symptoms following COVID-19 infection characterized by fatigue, shortness of breath, palpitations.⁵ These symptoms, in the setting of non-established cardiovascular disease, has been termed post-acute sequelae of COVID-19 cardiovascular syndrome, or PASC-CVS.⁶ The underlying mechanisms of the reported PASC-CVS remain uncertain. Coronary circulatory dysfunction has been suggested as potential functional substrate for cardiovascular post COVID-19 symptoms. COVID-19 may mediate adverse effects on the vasculature owing to both direct cytotoxic effect of the virus on the endothelium and/or the high levels of cytokines and other inflammatory markers, leading to an inflamed endothelium, platelet activation, leucocyte adhesion, and reduced nitric oxide bioavailability.⁵

Assessment of left-ventricular (LV) myocardial blood flow (MBF) during pharmacologically stimulated hyperemia, at rest and the resulting myocardial flow reserve (MFR) with positron emission tomography (PET) is used clinically to evaluate for the presence of coronary microvascular dysfunction as potential functional substrate for microvascular angina.^{7–9} Such noninvasively obtained information on hyperemic MBFs and MFR is also known to provide important prognostic information in patients with and without clinically-manifest coronary artery disease, ischemic and nonischemic cardiomyopathy.^{8,10} More recently, PET flow assessment of an abnormal decrease in MBF from the base to the apex of the left ventricle during hyperemic flows, a so-called longitudinal flow gradient, has been applied to provide more detailed information on functional and/or structural alterations of epicardial artery in individuals with cardiovascular risk.^{11,12} In the absence of structural alterations of the epicardial artery, the PET-determined longitudinal MBF gradient during hyperemic stimulation has been demonstrated to be related to an impairment of flow-mediated and, thus, endothelium-dependent epicardial vasodilation.¹¹ Taken together, it is intriguing to hypothesize that an abnormal function of the coronary circulation may provide a mechanistic link for the reported PASC-CVS. In this end, we aimed to evaluate whether PASC-CVS is associated with alterations in

coronary circulatory function as determined noninvasively with PET.

2 | METHODS

2.1 | Study population

The study population implied a subset of patients with post COVID-19 syndrome (post COVID-19-S) who had cardiovascular symptoms. Post COVID-19-S is defined as persistence of symptoms such as fatigue, shortness of breath, palpitations, and chest pain beyond 3 months of SARS-CoV-2 infection, lasting for at least 2 months and not explained by any other illness.⁵ PASC-CVS is defined as a heterogenous disorder of cardiovascular symptoms without evidence of cardiovascular disease that persist beyond the typical timeframe for infection and projected recovery based on the person's age and health status.^{5,6} Overall, the study population consisted of 23 patients with post COVID-19 syndrome/PASC-CVS and without known cardiovascular risk factors such as smoking, arterial hypertension (arterial blood pressure $\geq 140/90$ mmHg), hypercholesterolemia (fasting total serum cholesterol ≥ 240 mg/dL), and/or type 2 diabetes mellitus (fasting plasma glucose concentrations ≥ 126 mg/dL), respectively, who were consecutively referred for myocardial perfusion imaging with ¹³N-ammonia and PET/CT (Biograph mCT scanner, Siemens Healthineers) for evaluation of coronary circulatory function (Table 1). The primary reason for evaluation of coronary circulatory with PET/CT was ongoing chest pain, while other symptoms such as fatigue, shortness of breath, and/or palpitations may have co-existed. In addition, 23 healthy patients without or with medically controlled cardiovascular risk factors underwent the same imaging protocol and served as control group. Excluded were patients with a history of acute coronary syndrome or myocardial infarction, hypertrophic obstructive and nonobstructive cardiomyopathy, congestive heart failure, malignant hypertension (defined as diastolic blood pressure > 120 mm Hg with the presence of severe hypertensive retinopathy and organ damage), valvular heart disease, anemia, or endocrine, hepatic, renal, or non-COVID 19 inflammatory disease. Further, only individuals with normal stress–rest perfusion imaging and wall motion analysis, as determined by gated ¹³N-ammonia PET/CT that widely excluded the presence of hemodynamically significant obstructive CAD, served for study purpose. In all study patients, echocardiography demonstrated normal thickness of the left ventricular wall (< 15 mm), wall motion, and valvular function. All patients with post COVID-19 syndrome had confirmed SARS-CoV-2 infection as determined with reverse

TABLE 1 Clinical characteristics, symptoms, and coronary artery calcifications of the study population

	Controls	PASC-CVS	<i>p</i> Values
Gender (male/female)	10/13	2/21	.006
Age (years)	56 ± 12	46 ± 11	.001
BMI (kg/m ²)	26 ± 2.5	30 ± 5.7	.006
Symptoms			
Typical angina	8 (35)	17 (74)	.007
Atypical angina	15 (65)	6 (26)	.007
Dyspnea	9 (39)	12 (52)	.386
Palpitations	3 (13)	13 (57)	.001
Risk Factors			
Hypertension (<i>n</i>)	4 (17)	0	.160
Smoking (<i>n</i>)	0	0	/
Obesity (<i>n</i>)	0	11 (47)	.0001
Hypercholesterolemia (<i>n</i>)	5 (21)	0	.017
Family history of CAD (<i>n</i>)	0	0	/
Diabetes mellitus (<i>n</i>)	0	0	/
Fasting Plasma Concentrations			
Cholesterol, mg/dl	172 ± 36	198 ± 31	.003
LDL, mg/dl	105 ± 38	119 ± 26	.009
HDL, mg/dl	54 ± 12	57 ± 12	.860
TG, mg/dl	99 ± 35	109 ± 53	.773
Glucose, mg/dl	94 ± 8	87 ± 8	.060
HbA1c, %	5.4 ± 0.13	5.3 ± 0.14	.721
hsCRP, mg/dl	1.35 ± 0.98	6.19 ± 6.63	.008
Coronary artery calcifications			
CCS	1.30 + 1.70	0.30 + 1.11	.081
CCS, median (IQR)	0 (0.0)	0 (0.0)	/

Note: Values are mean ± SD, for coronary calcium score (CCS) additional median and interquartile range (Q1,Q3) is indicated; *p* values versus controls (Mann–Whitney *U* test for independent samples).

Abbreviations: CCS, coronary calcium score; HbA1c, hemoglobin A1c; HDL, high-density lipoprotein; hsCRP, high sensitive C-reactive protein; LDL, low-density lipoprotein; n (%), numbers; PASC-CVS, Post-acute sequelae of COVID-19 cardiovascular syndrome; TG, triglyceride.

transcription- polymerase chain reaction (RT-PCR) swab test but normal troponin I levels. The mean time from PCR confirmed SARS-CoV-2 infection was 332 ± 130 days. Patients with PASC-CVS commonly reported symptoms of chest tightness, palpitations and shortness of breath.⁵ Any vasoactive medications such as calcium channel blockers, angiotensin-converting enzyme inhibitors, nitroglycerin, and/or b-blockers to treat symptoms were discontinued at least 24 h before PET/CT perfusion and flow study. All study participants refrained from caffeine-containing beverages for ≥24 h prior to the PET study. The study was approved by the Institutional Review Board of the Washington University in St. Louis (No.201812037 and 202,004,077), and each participant signed a clinical approved informed consent form. Reporting of the study conforms to broad EQUATOR guidelines.¹³

2.2 | Cardiac PET/CT flow assessment

Following the topogram used to determine the axial field of view and a low-dose CT scan (120 kV, 30 mA) for attenuation correction, ¹³N-ammonia PET determined myocardial perfusion and MBF in mL/min/g with serial image acquisition and a two-compartment tracer kinetic model during regadenoson-stimulated hyperemia and at rest, respectively.^{7,11} PET image acquisition was performed during regadenoson-stimulated hyperemia (0.4 mg intravenous bolus injection over 10 and 20 s interval) was started immediately following injection of ≈370 MBq ¹³N-ammonia as a bolus followed with immediate infusion of 10 ml saline solution over 30 sec (0.33 ml/sec) via fusion pump (e.g. Aitecs Syringe Pump) and also 40 min later at rest for a total duration of 10 min list-mode PET data

acquisition, respectively. Myocardial perfusion images during pharmacologic-induced hyperemia and at rest were evaluated visually on reoriented short- and long-axis myocardial slices and semiquantitatively on the corresponding polar map from the last static 10 min transaxial PET image. Semiquantitative evaluation of ^{13}N -ammonia PET perfusion images was performed with a standard 17-segment model and a five-point grading system by two expert observers.¹¹ Summed stress score (SSS), summed rest score (SRS), and summed difference score (SDS) were determined. A SDS ≥ 2 signified a reversible perfusion defect, whereas < 2 was deemed as normal. Accordingly, patients with a SDS ≥ 2 , suggestive of hemodynamically obstructive CAD lesions, were excluded from study analysis. For quantification of myocardial blood flow in ml/g/min, left ventricular (LV) contours and input function region were obtained automatically with minimal operator intervention using Corridor4DM software (Cardiac; 4DM PET CFR) version 2016 (INVIA Medical Imaging Solutions, Ann Arbor, MI).⁷ Regional MBFs of the three main myocardial vascular territories subtended to the left anterior descending artery (LAD), left circumflex artery (LCx), and right coronary artery (RCA) were averaged on a polar map, and the resulting mean MBF of the LV was defined as global MBF.⁷ Following, longitudinal flows, MBFs in the mid and mid-distal myocardial segment of the LV corresponding to the vascular territories of the LAD (segments: 7–8 and 13–14), LCx (segments: 11–12 and 16), and RCA (segments: 9–10 and 15) were determined.¹¹ Basal segments (LAD: 1–2, LCx: 5–6, and RCA: 3–4) and the apical segment (LAD: 17), however, were not included for this analysis owing to a possible count variability induced by the membranous septum, by a certain variability in locating the last apical slice, and by partial volume errors resulting from object size at the apex.^{11,12,14} Heart rate, blood pressure, and a 12-lead electrocardiogram were recorded at baseline and after regadenoson application continuously during MBF measurement. From the average of heart rate and systolic blood pressure during the first 2 min at baseline and after regadenoson application, the rate-pressure product (RPP = heart rate \times systolic blood pressure) was derived as an index of myocardial workload. A decrease in MBF from mid to mid-distal LV myocardium (ml/g/min) was defined as longitudinal, base-to-apex MBF gradient. Changes in the longitudinal, base-to-apex MBF gradient from rest to regadenoson-stimulated hyperemia were defined as rest-to-stress change in longitudinal, base-to-apex MBF gradient (Δ longitudinal MBF gradient = longitudinal MBF gradient during hyperemia minus longitudinal MBF gradient at rest). To account for inter-individual variations in coronary driving pressure, an index of coronary vascular resistance (CVR) was determined as the ratio of mean

arterial blood pressure (mmHg) to MBF (ml/g/min). As resting MBF is dependent on the myocardial workload, it was normalized to the RPP (averaged during the first 2 min of image acquisition; MBF divided by RPP multiplied by 10,000). This again served to calculate the corrected MFR (Hyperemic MBF during regadenoson divided by NMBF at rest). The left ventricular ejection fraction (LVEF) during peak stress and at rest was evaluated by gated PET. A normal LVEF was considered $> 45\%$. LVEF reserve was studied in clinically relevant categories of ($\leq 0\%$ denoting no increase or decrease in LVEF with stress) versus $> 0\%$ (increase in LVEF with stress).¹⁵ A visual four-point scoring system was used to indicate coronary artery calcifications (0 = normal, 1 = mild, 2 = moderate, and 3 = severe calcifications) of the LAD, LCx, and RCA on the nongated and low-dose CT for attenuation correction.¹⁶ From all three coronary vessels the mean coronary calcium score (CCS) was calculated.

2.3 | Statistical analysis

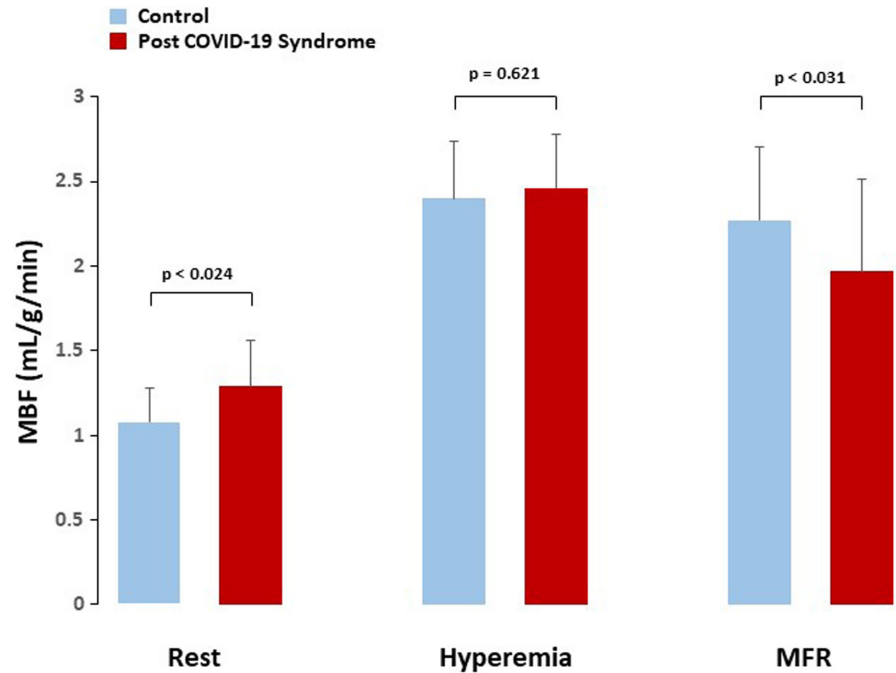
Data are presented as the mean \pm SD for quantitative and absolute frequencies for qualitative variables. For comparison of differences, appropriate t-tests for independent or paired samples were used. A comparison of regadenoson-related MBFs and MFR among the different groups was performed by 1-way analysis of variance (ANOVA) followed by Scheffe multiple comparison test. Since coronary calcium scores (CCS) followed a pronounced skewed distribution, there are also presented as median and interquartile range (25th to 75th percentile: Q1,Q3). Pearson's correlation coefficients (r), assuming a linear regression and the standard error of the estimate (SEE), were calculated to investigate possible associations among MBF, hemodynamic, post COVID-19 syndrome interval, and high sensitive C-reactive protein, respectively. Differences in LVEF reserves were analysed with the χ^2 test. All test procedures were 2-tailed, and $p \leq .05$ was considered statistically significant. All statistical analyses were performed with SPSS for Windows 25.0 (SPSS).

3 | RESULTS

3.1 | Clinical characteristics

Table 1 describes the characteristics and symptoms of the study population. PASC-CVS group consisted predominantly of female patients and body mass index was higher when compared with controls. Typical angina was more prevalent than atypical angina in the PASC-CVS compared with the control group, while it was the

FIGURE 1 Myocardial blood flow (MBF) at rest, during regadenoson-stimulated hyperemia, and corresponding myocardial flow reserve (MFR) for both study groups



opposite for atypical angina. Palpitations manifested more frequently in the PASC-CVS than in the control group, while there were no differences for dyspnea between both groups. As regards total cholesterol and LDL levels, they were within normal range but higher in PASC-CVS than in controls. Further, high-sensitive C-reactive protein (CRP) plasma levels were significantly elevated in PASC-CVS than in controls. In the control group, four individuals had medically controlled arterial blood pressure regulation. They were treated with B-blocker ($n = 1$), angiotensin-converting enzyme inhibitor ($n = 2$), diuretics ($n = 1$), and calcium-channel blocker ($n = 1$) (Table 1). In addition, five control individuals were on statin medication with total cholesterol serum levels in normal range. In the PASC-CVS group without known cardiovascular risk factors, eleven patients were obese with a BMI ranging between 31.2–38.6 kg/m². As regards the presence of coronary artery calcifications in the PASC-CVS group, only two individuals had appreciable calcifications in three and two coronary vessels, respectively. Conversely, in controls, nine individuals had appreciable calcifications in one vessel ($n = 4$), two vessels ($n = 3$), and three vessels ($n = 2$), respectively. The CCS score, tended to be lower in the PASC-CVS group when compared with controls, while it did not reach statistical significance (Table 1). Further, the average time between first to second radiotracer injections of ¹³N-ammonia was 63 ± 11 min that should have widely avoided interference of residual myocardial ¹³N-ammonia activity from the first injection with the second ¹³N-ammonia injection for the rest myocardial perfusion scan.

3.2 | Hemodynamics and global flows

For the whole study group, hemodynamics at baseline and 10 min after regadenoson application did not differ significantly (heart rate: 71 ± 10 vs. 72 ± 9 and SBP: 126 ± 8 vs. 127 ± 8 mmHg; $p = .848$ and $p = .770$, respectively), widely excluding regadenoson-induced transient changes in hemodynamics on subsequent hemodynamics after the 10 min interval. While resting heart rate (HR), systolic blood pressure (SBP), and corresponding rate-pressure product (RPP) were similar among groups, MBF was significantly higher in PASC-CVS than in controls (Table 1). When resting MBF was normalized to the RPP, the normalized MBF was also higher in PASC-CVS compared with controls suggestive of some uncoupling of the resting MBF from the myocardial workload. During regadenoson-stimulated hyperemia, HR increased significantly from rest in both groups, while being significantly higher in PASC-CVS. Conversely, there was a significant and comparable decrease in SBP during regadenoson-stimulation from rest among groups. The RPP during pharmacologic vasodilation and hyperemic MBFs did not differ significantly among groups (Figure 1). When the hyperemic MBF was related to the mean arterial blood pressure in order to compensate for possible interindividual variations in coronary driving pressure, the resulting estimates of CVR widely mirrored the global MBF values during pharmacologic vasodilation for each group studied and thus were comparable (Table 2). MFR and global corrected MFR, however, were significantly less in PASC-CVS than in controls, respectively (Table 2) (Figure 3). The group comparison of the MFR and corrected MFR among did

	Controls	PASC-CVS	p Value
Flow Parameters			
MBF- Rest	1.08 ± 0.20	1.29 ± 0.27	.024
NMBF-Rest	1.25 ± 0.17	1.40 ± 0.32	.073
MBF-Stress	2.40 ± 0.34	2.46 ± 0.53	.621
MFR	2.27 ± 0.43	1.97 ± 0.54	.031
Corrected MFR	1.98 ± 0.63	1.55 ± 0.77	.014
CVR-Rest	88 ± 25	77 ± 18	.055
CVR-Stress	32 ± 5	36 ± 8	.652
MBF Gradient-Rest	-0.01 ± 0.07	-0.03 ± 0.10	.675
MBF Gradient-Stress	0.03 ± 0.13	-0.20 ± 0.19	.000
ΔMBF Gradient	0.04 ± 0.11	-0.17 ± 0.18	.000
CVR Gradient-Rest	1.19 ± 4.04	1.19 ± 3.52	.912
CVR Gradient-Stress	-0.06 ± 0.81	2.66 ± 2.86	.000
ΔCVR Gradient	-1.25 ± 4.00	1.47 ± 4.08	.030
Hemodynamics			
Rest-HR, bpm	71 ± 12	73 ± 10	.403
Stress-HR bpm	98 ± 16	110 ± 12	.004
Rest-SBP, mmHg	125 ± 10	129 ± 8	.071
Stress-SBP, mmHg	112 ± 12	116 ± 7	.474
Rest-RPP	8966 ± 1969	9374 ± 1320	.385
Stress-RPP	11.078 ± 2640	12.714 ± 1358	.007
LVEF (%)			
Stress	49.7 ± 3.7	51.4 ± 4.3	.268
Rest	49.3 ± 2.7	50.8 ± 3.6	.127
Reserve (Stress-Rest)	0.39 ± 3.2	0.26 ± 3.1	.890
Reserve ≤ 0	-2.09 ± 1.70	-1.64 ± 1.91	.541
Reserve > 0	2.66 ± 2.53	3.22 ± 2.17	.595

Note: Values are mean ± SD; p values versus controls (Mann-Whitney *U* test for independent samples).

Abbreviations: corrected MFR, ratio MBF-DP to NMBR at rest; CVR, coronary vascular resistance (mmHg/ml/g/min); HR, heart rate; MBF, myocardial blood flow (ml/g/min); NMBF, normalized MBF (ml/g/min), MFR, myocardial flow reserve; RPP, rate-pressure product (HR x SBP); SBP, systolic blood pressure; LVEF, left ventricular ejection fraction.

not reach statistical significance ($p = .063$ and $p \leq .073$ by ANOVA, respectively). We also investigated the relationship between MBF and RPP at rest. As it was observed, the resting MBF closely correlated with the corresponding RPP in controls ($r = 0.758$, $SEE = 0.136$, $p < .0001$) but not in PASC-CVS ($r = 0.093$, $SEE = 0.273$, $p = .673$), implying a certain uncoupling of the resting MBF from the metabolic demand in PASC-CVS.

Finally, the LVEF during peak stress, at rest, and corresponding reserve (LVEF stress-LVEF rest) did not differ between both groups (Table 2). An abnormal LVEF reserve was observed in 14 (61%) and in 9 (39%) and normal LVEF reserve in 11 (48%) and 12 (52%) cases in the PASC-CVS and control group, respectively ($p = .375$). Further, we evaluated a potential association between LVEF reserve and MFR in the study

TABLE 2 Myocardial flow parameters, hemodynamics, and function in controls and in post-acute sequelae of COVID-19 cardiovascular syndrome (PASC-CVS) patients during PET/CT

group as a whole, PASC-CVS, and controls, respectively, but no significant correlations were noted ($r = 0.029$, $SEE = 3.175$, $p = .850$; $r = 0.006$, $SEE = 3.195$, $p = .980$; and $r = 0.088$, $SEE = 3.292$, and $p = .690$). Further, when looking at associations between the abnormal LVEF reserve ($\leq 0\%$) and MFR in the PASC-CVS and controls group, respectively, no significant correlations were observed ($r = 0.093$, $SEE = 1.974$, $p = .751$ and $r = 0.584$, $SEE = 1.454$, $p = .059$).

3.3 | Longitudinal, base-to-apex MBF gradient

Resting regional MBF was tended to be mildly and non-significantly less in the mid-distal than in the mid-LV

myocardium in both groups of PASC-CVS and controls (1.36 ± 0.25 vs. 1.39 ± 0.29 and 1.19 ± 0.23 vs. 1.20 ± 0.22 ml/g/min, $p = .114$ and $p = .404$, respectively). This resulted in very small and comparable longitudinal decrease in flow at rest between both groups (Table 2). During hyperemic MBFs, there was a marked and significant decrease in longitudinal MBF from the base to apex direction in PASC-CVS, not observed in controls (2.77 ± 0.57 vs. 2.56 ± 0.56 and 2.60 ± 0.39 vs. 2.63 ± 0.38 ml/g/min, respectively, $p \leq .0001$ and $p = .299$, respectively), which resulted in a marked longitudinal MBF gradient during pharmacologic vasodilation and Δ longitudinal MBF gradient in PASC-CVS, respectively (Table 2) (Figure 2). Similarly, the calculation of the longitudinal CVR gradients at rest, during pharmacologic stress, and the Δ longitudinal CVR gradient paralleled longitudinal MBF values for both groups studied (Table 2) widely excluding confounding effects of inter-individual variations in coronary driving pressure. The group comparison of the Δ longitudinal MBF and CVR gradient in PASC-CVS was significant compared with controls ($p < .0001$ and $p \leq .044$ by ANOVA, respectively). Further, in order to account for possible confounding effects of obesity in the PASC-CVS group, a sub analysis of the hyperemic longitudinal MBF gradient in nonobese individuals was performed. The longitudinal MBF gradient during pharmacologic vasodilation and Δ longitudinal MBF gradient in nonobese PASC-CVS patients, respectively, persisted and they did not differ significantly when compared with the whole PASC-CVS group (-0.26 ± 0.21 vs. -0.20 ± 0.19 and -0.21 ± 0.22 vs. -0.17 ± 0.18 ml/g/min, $p = .441$ and $p = .554$, respectively) (Table 2).

3.4 | Correlation between MBFs, high-sensitive CRP, and post-COVID interval

The regression analysis between elevated high-sensitive C-reactive protein (hsCRP) levels and MBFs at rest, during hyperemia, and corresponding MFR did not demonstrate statistically significant correlations in PASC-CVS ($r = 0.209$, SEE = 0.281, $p = .362$; $r = 0.010$, SEE = 0.547, $p = .967$; and $r = 0.140$, SEE = 0.561, $p = .546$). Further, we evaluated a potential association between hsCRP levels and the longitudinal MBF gradient at rest, during hyperemia, and the Δ longitudinal MBF gradient that did not yield any significant associations in PASC-CVS ($r = 0.065$, SEE = 0.099, $p = .779$; $r = 0.046$, SEE = 0.195, $p = .843$; and $r = 0.082$, SEE = 0.191, $p = .723$). Finally, we aimed to evaluate possible associations between the PASC-CVS interval and MBFs at rest, during hyperemia, and corresponding MFR did not demonstrate statistically significant correlations ($r = 0.010$, SEE = 0.273, $p = .963$; $r = 0.093$, SEE = 0.541, $p = .673$; and $r = 0.136$, SEE = 0.543, $p = .537$). Similarly, the regression analysis between the disease interval in PASC-CVS and the longitudinal MBF gradient at rest, during hyperemia, and the Δ longitudinal MBF gradient did not demonstrate significant associations, respectively ($r = 0.293$, SEE = 0.092, $p = .175$; $r = 0.002$, SEE = 0.193, $p = .991$; and $r = 0.150$, SEE = 0.188, $p = .494$).

4 | DISCUSSION

The present study provides several unique observations of coronary circulatory function in patients with PASC-CVS.

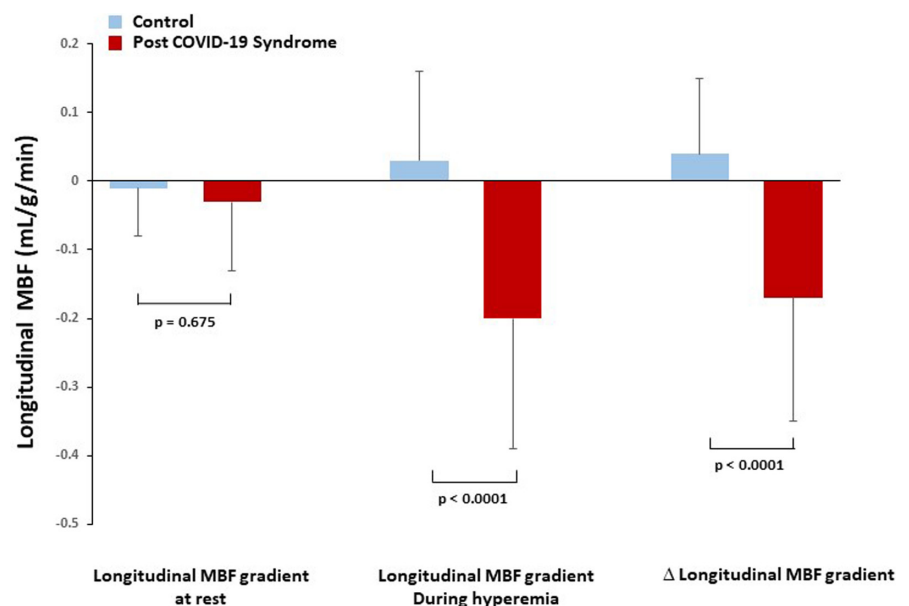


FIGURE 2 Δ longitudinal myocardial blood flow (MBF) gradient (longitudinal MBF gradient during hyperemia minus longitudinal MBF gradient at rest) for both two study groups

First, post COVID syndrome may be associated with an abnormal hyperemic longitudinal MBF gradient, which has been related to an impairment of flow-mediated epicardial vasodilation and thus, at least in part, to alterations in endothelium-dependent vasodilator mechanisms. As an impairment of flow-mediated epicardial vasodilation may confer a worse clinical outcome,^{8,10} the observed dysfunction of flow-mediated epicardial vasodilation may pose a future risk for adverse cardiovascular outcomes in PASC-CVS patients that remains to be evaluated clinically. Second, hyperemic MBFs were comparable between patients with PASC-CVS and healthy controls signifying a widely preserved function of the coronary arteriolar vessels. Third, reductions in coronary vasodilator capacity are predominantly related to increases in resting flow in PASC-CVS when compared with healthy controls needing further investigations.

PET/CT-determined resting MBFs in PASC-CVS patients were observed to be significantly higher than in controls. This is somehow surprising as resting heart rates, SBP's and resulting RPP, indicative of the myocardial workload, were comparable among groups and someone would have expected comparable resting MBFs according to the metabolic demand. In this respect, there was a significant and positive correlation between the resting MBF and corresponding RPP in control individuals emphasizing the coupling of the resting MBF to the RPP as described previously.¹⁷ Conversely, no such correlation between resting MBF and RPP was observed any more in PASC-CVS patients. Thus, it appears that the observed higher resting MBFs in PASC-CVS patients when compared with controls does not appear to be determined only by the myocardial workload but may be related, at least in part, to an additional activation of the sympathetic nervous system and/or renin-angiotensin-aldosterone system as described previously.¹⁸ This would also agree with the PASC-CVS patients having presented an excessive tachycardic response to minimal exertion during treadmill exercise and/or during pharmacologic stress for the PET/CT study suggestive of some cardiac dysautonomia or excitability. Conceptually, gender differences may also have added, at least in part, to observed higher resting in the PASC-CVS group that predominantly consisted of female patients when compared with the control group with balanced gender distribution.¹⁹ Interestingly, higher hyperemic MBF in female than in male has also been described previously,¹⁹ that was attributed to a more favorable lipid profile seen in women than in men. In this respect, someone would have expected higher hyperemic MBFs in PASC-CVS than in controls but they were comparable in the current study. This raises an interesting speculation that the PASC-CVS group may indeed have some mild reductions hyperemic MBFs when the predominance

of female patients is taken into account that warrants further testing in a larger cohort and more gender specific investigation.

In the current study, we included only post COVID syndrome individuals without known cardiovascular risk factors such as smoking, arterial hypertension, hypercholesterolemia, and/or type 2 diabetes mellitus to avoid confounding effects of these factors on coronary circulatory function. Interestingly, averaged hyperemic MBFs were in normal range and comparable among both groups signifying a widely normal functioning of the vascular smooth muscle cells of the coronary arteriolar vessels. Consequently, the observed marked decrease in total coronary vasodilator capacity in PASC-CVS compared with controls can be related predominantly to increase in resting MBFs that put forth an impairment of the endogenous type of the myocardial flow reserve as potential functional substrate for reported angina symptoms. Such possibility is supported by recent assessment of myocardial perfusion and MBF with ⁸²rubidium PET/CT in 1515 symptomatic patients with known or suspected CAD.¹⁵ Impaired augmentation of left ventricular ejection fraction and myocardial blood flow were indeed independently associated with angina symptoms and dyspnea, respectively.¹⁵ This may agree somehow with current observations that unraveled an impaired augmentation of left ventricular ejection fraction with pharmacologic stress in about 50%–60% of symptomatic patients. Conversely, we did not find a significant association between impaired increase in left ventricular ejection fraction and myocardial flow reserve in the whole study group, PASC-CVS, and control patients, respectively. The reason for the in part discordant observation between the current and recent investigation¹⁵ remains uncertain but are likely to be related to differences in hyperemic flows that were widely normal in the current study, differences in patient's characteristics as well as in sample size studied. It is also possible that the current study population was not large enough or, conversely, that the range of impaired increase in left ventricular ejection fraction was not wide enough to unravel a statistically significant association. Notably, PASC-CVS patients had significantly more typical angina than in controls in the absence of obstructive CAD. In this regard, it is important to note that the observed abnormal hyperemic longitudinal MBF gradient requires a parallel associated longitudinal pressure gradient that reduced subendocardial perfusion.^{20,21} Thus, the observed hyperemic longitudinal MBF gradient in conjunction with a certain stress-induced sympathetic overdrive may indeed account for reductions in subendocardial flow or ischemia, despite the absence of flow-limiting CAD, potentially reflecting a functional substrate for observed typical angina.²¹ PASC-CVS with persistent

systemic inflammation has been linked to an impairment of flow-mediated and thus endothelium-dependent function of the brachial artery.^{22,23} The results of the current study provide the first evidence that PASC-CVS is also associated with an impairment of flow-mediated epicardial vasodilation as demonstrated by a PET-determined abnormal longitudinal MBF gradient during hyperemic stimulation not observed in controls. These findings may also explicitly link epicardial endothelial dysfunction to alpha sympathetic activation causing mild diffuse epicardial vasoconstriction despite increases in coronary blood flow due to inotropic demand or pharmacologic vasodilation of the coronary arteriolar vessels.^{10,24} The mild sympathetic coronary constriction at hyperemic flow in the presence of endothelial dysfunction preventing epicardial vasodilation then causes the longitudinal MBF gradient during normal hyperemic microvascular response to pharmacologic vasodilation. Since the PASC-CVS group, however, had a substantial portion of obese patients, the abnormal hyperemic longitudinal MBF gradient may have been related also in part to adverse effects of obesity on coronary circulatory function. When obese PASC-CVS patients were excluded from analysis, however, the abnormal hyperemic longitudinal MBF gradient was quite comparable to the whole PASC-CVS group ruling out significant adverse effects of obesity on flow-mediated epicardial vasodilation in these patients. Another factor worthy of considerations is CAD related structural alterations or vessel stiffness that may prevent an appropriate flow-mediated epicardial vasodilation during hyperemic flows increases causing an abnormal longitudinal perfusion or flow gradient.²⁵ Thus, apart from a mild sympathetically-mediated epicardial vasoconstriction in the presence of a dysfunctional endothelium, nonobstructive diffuse CAD may have contributed to the manifestation of the hyperemic longitudinal MBF gradient in PASC-CVS patients. Mild to-moderate coronary artery calcifications as a surrogate for CAD plaque burden as determined on low-dose CT, however, was present only in two and nine patients in the PASC-CVS and control group, respectively. Semi-quantitatively evaluated coronary artery calcium score¹⁶ was low albeit it tended to be higher in controls without an abnormal hyperemic longitudinal MBF gradient that was observed in PASC-CVS patients. These findings may signify a functional impairment of flow-mediated epicardial vasodilation as predominant cause for the observed abnormal hyperemic longitudinal MBF gradient in PASC-CVS in the current study.

Interestingly, we did not observe an association between elevated hsCRP levels and impairment of flow-mediated epicardial vasodilation in PASC-CVS as reported previously for individuals with cardiovascular risk factors.²⁴ As hsCRP levels reflect systemic micro-inflammation, more

specific parameters of the SARS-CoV-2 infection related to acute and chronic immune and inflammatory response are likely to account for the PET-determined impairment of flow-mediated epicardial vasodilation that, however, warrants further investigations. In patients with cardiovascular risk factors, inflammation of the arterial wall favors pro-atherosclerotic effects such as the expression of endothelial cell adhesion molecules, the production of chemo-attractant chemokines, the macrophage LDL uptake, and the downregulation of endothelial nitric oxide synthase expression that confers a worse cardiovascular outcome.²⁶ For the time being, however, it remains uncertain whether the observed impairment of flow-mediated epicardial vasodilation is an additional mediator for the initiation and/or acceleration of structural CAD in individuals with cardiovascular risk factors or just a transient phenomenon of no pathological consequence. Also unknown is whether pharmacologic treatment with beta blockers to reduce the effects of sympathetic activation and/or vasodilators lead to changes over time in these findings. Of further interest, we did not observe an association between PASC-CVS interval and PET-determined impairment of flow-mediated epicardial vasodilation. Thus, it appears that PASC-CVS related severity of diminished flow-mediated epicardial vasodilation is widely constant and likely sustained by a chronic immune-modulatory and inflammatory response.²⁷⁻³⁰

4.1 | Limitations

There are important limitations worthy of consideration. In view of the relatively small sample size of patients with PASC-CVS and healthy volunteers, current findings may be seen more as a “proof principle” study. On the other hand, these initial observations may provide an important framework to initiate larger clinical trials to draw more definite conclusions for alterations in coronary circulatory function in PASC-CVS. Further, albeit that the half-life of the initial phase of the intravenously stressor regadenoson is approximately 2–4 min, the subsequent intermediate phase follows with an average half-life 30 min converging with the loss of pharmacodynamics effects. Thus, some residual influence of regadenoson activation on hemodynamics measured 10 min after intravenous injection cannot be excluded but it should have been similar for both groups studied. MBFs in the mid and mid-distal left-ventricular segments were measured and, thus, the longitudinal MBF gradient was determined over a relatively short longitudinal distance aiming to avoid confounding count variability in the basal segments and partial volume effects in the apical segment on MBF measurements. This again

likely has manifested in some underestimation of the longitudinal MBF gradient during hyperemic flow stimulation. In this direction, myocardial flow assessment on a voxel-basis²⁵ likely would have allowed a more accurate measure of the observed longitudinal MBF gradient during hyperemic flows in PASC-CVS patients.

In conclusion, in PASC-CVS, coronary vascular alterations were largely confined to an impairment of flow-mediated epicardial vasodilator mechanisms and had not yet affected vascular smooth muscle cell function. Whether such an impairment of flow-mediated epicardial vasodilation confers an increased risk for future cardiovascular events in PASC-CVS with or without pre-existing CAD remains to be clinically tested. Further, PASC-CVS was associated with reductions in coronary vasodilator capacity predominantly related to increases in resting MBFs or “endogen type” of altered myocardial flow reserve warranting further clinical investigations.

AUTHOR CONTRIBUTIONS

All authors have a substantial contribution in the conception and design of the study, participated in analysis and interpretation of data, and drafted the manuscript. TS, AV and IV have a substantial contribution to the conception and design of the study and revising the manuscript for intellectual content. ML, AU, TR, JM, FD, RG, and PW participated in study conception, and in revision of the manuscript.

ACKNOWLEDGEMENTS

This study was supported by a departmental fund from Washington University in St. Louis.

FUNDING INFORMATION

Departmental fund from Washington University in St. Louis.

CONFLICT OF INTEREST

The authors declare that they have no known competing financial interests or personal relationships that could have appeared to influence the contents of this manuscript.

RELATIONSHIP WITH INDUSTRY

None.

ORCID

Thomas Hellmut Schindler  <https://orcid.org/0000-0002-2141-7716>

REFERENCES

- Guan WJ, Ni ZY, Hu Y, et al. Clinical characteristics of coronavirus disease 2019 in China. *N Engl J Med*. 2020;382:1708-1720.
- Lip GYH, Genaidy A, Tran G, Marroquin P, Estes C, Sloop S. Effects of multimorbidity on incident COVID-19 events and its interplay with COVID-19 event status on subsequent incident myocardial infarction (MI). *Eur J Clin Invest*. 2022;52:e13760.
- Melillo F, Napolano A, Loffi M, et al. Myocardial injury in patients with SARS-CoV-2 pneumonia: pivotal role of inflammation in COVID-19. *Eur J Clin Invest*. 2022;52:e13703.
- Masetti C, Generali E, Colapietro F, et al. High mortality in COVID-19 patients with mild respiratory disease. *Eur J Clin Invest*. 2020;50:e13314.
- Raman B, Bluemke DA, Luscher TF, Neubauer S. Long COVID: post-acute sequelae of COVID-19 with a cardiovascular focus. *Eur Heart J*. 2022;43:1157-1172.
- Writing C, Gluckman TJ, Bhavne NM, et al. 2022 ACC expert consensus decision pathway on cardiovascular sequelae of COVID-19 in adults: myocarditis and other myocardial involvement, post-acute sequelae of SARS-CoV-2 infection, and return to play: a report of the American College of Cardiology Solution set Oversight Committee. *J Am Coll Cardiol*. 2022;79:1717-1756.
- Upadhyaya A, Bhandiwad A, Lang J, et al. Coronary circulatory function with increasing obesity: a complex U-turn. *Eur J Clin Invest*. 2022;52:e13755.
- Schindler TH, Dilsizian V. Coronary microvascular dysfunction: clinical considerations and noninvasive diagnosis. *JACC Cardiovasc Imaging*. 2020;13:140-155.
- Schindler TH, Bateman TM, Berman DS, et al. Appropriate use criteria for PET myocardial perfusion imaging. *J Nucl Med*. 2020;61:1221-1265.
- Schindler TH, Schelbert HR, Quercioli A, Dilsizian V. Cardiac PET imaging for the detection and monitoring of coronary artery disease and microvascular health. *JACC Cardiovasc Imaging*. 2010;3:623-640.
- Valenta I, Antoniou A, Marashdeh W, et al. PET-measured longitudinal flow gradient correlates with invasive fractional flow reserve in CAD patients. *Eur Heart J Cardiovasc Imaging*. 2017;18:538-548.
- Valenta I, Quercioli A, Schindler TH. Diagnostic value of PET-measured longitudinal flow gradient for the identification of coronary artery disease. *JACC Cardiovasc Imaging*. 2014;7(4):387-396.
- Simera I, Moher D, Hoey J, Schulz KF, Altman DG. A catalogue of reporting guidelines for health research. *Eur J Clin Invest*. 2010;40:35-53.
- Gould KL, Nakagawa Y, Nakagawa K, et al. Frequency and clinical implications of fluid dynamically significant diffuse coronary artery disease manifest as graded, longitudinal, base-to-apex myocardial perfusion abnormalities by noninvasive positron emission tomography. *Circulation*. 2000;101:1931-1939.
- Patel KK, Peri-Okonny PA, Qarajeh R, et al. Prognostic relationship between coronary artery calcium score, perfusion defects, and myocardial blood flow Reserve in Patients with Suspected Coronary Artery Disease. *Circ Cardiovasc Imaging*. 2022;15:e012599.
- Einstein AJ, Johnson LL, Bokhari S, et al. Agreement of visual estimation of coronary artery calcium from low-dose CT attenuation correction scans in hybrid PET/CT and SPECT/CT with standard Agatston score. *J Am Coll Cardiol*. 2010;56:1914-1921.

17. Czernin J, Muller P, Chan S, et al. Influence of age and hemodynamics on myocardial blood flow and flow reserve. *Circulation*. 1993;88:62-69.
18. Quercioli A, Pataky Z, Vincenti G, et al. Elevated endocannabinoid plasma levels are associated with coronary circulatory dysfunction in obesity. *Eur Heart J*. 2011;32:1369-1378.
19. Duvernoy CS, Meyer C, Seifert-Klauss V, et al. Gender differences in myocardial blood flow dynamics: lipid profile and hemodynamic effects. *J Am Coll Cardiol*. 1999;33:463-470.
20. Collet C, Sonck J, Vandeloos B, et al. Measurement of hyperemic pullback pressure gradients to characterize patterns of coronary atherosclerosis. *J Am Coll Cardiol*. 2019;74:1772-1784.
21. Gould KL. Apples, oranges, or pears: unexpected insights in coronary pathophysiology. *Eur Heart J Cardiovasc Imaging*. 2019;20:14-17.
22. Ratchford SM, Stickford JL, Province VM, et al. Vascular alterations among young adults with SARS-CoV-2. *Am J Physiol Heart Circ Physiol*. 2021;320:H404-H410.
23. Moretta P, Maniscalco M, Papa A, Lanzillo A, Trojano L, Ambrosino P. Cognitive impairment and endothelial dysfunction in convalescent COVID-19 patients undergoing rehabilitation. *Eur J Clin Invest*. 2022;52:e13726.
24. Schindler TH, Nitzsche EU, Olschewski M, et al. Chronic inflammation and impaired coronary vasoreactivity in patients with coronary risk factors. *Circulation*. 2004;110:1069-1075.
25. Gould KL, Johnson NP, Bateman TM, et al. Anatomic versus physiologic assessment of coronary artery disease. Role of coronary flow reserve, fractional flow reserve, and positron emission tomography imaging in revascularization decision-making. *J Am Coll Cardiol*. 2013;62:1639-1653.
26. Munzel T, Daiber A, Ullrich V, Mulsch A. Vascular consequences of endothelial nitric oxide synthase uncoupling for the activity and expression of the soluble guanylyl cyclase and the cGMP-dependent protein kinase. *Arterioscler Thromb Vasc Biol*. 2005;25:1551-1557.
27. Vdovenko D, Balbi C, Di Silvestre D, et al. Microvesicles released from activated CD4(+) T cells alter microvascular endothelial cell function. *Eur J Clin Invest*. 2022;52:e13769.
28. Jimeno S, Ventura PS, Castellano JM, et al. Prognostic implications of neutrophil-lymphocyte ratio in COVID-19. *Eur J Clin Invest*. 2021;51:e13404.
29. Garcia de Guadiana-Romualdo L, Calvo Nieves MD, Rodriguez Mulero MD, et al. MR-proADM as marker of endotheliitis predicts COVID-19 severity. *Eur J Clin Invest*. 2021;51:e13511.
30. Indirli R, Bandera A, Valenti L, et al. Prognostic value of copeptin and mid-regional proadrenomedullin in COVID-19-hospitalized patients. *Eur J Clin Invest*. 2022;52:e13753.

How to cite this article: Verma A, Ramayya T, Upadhyaya A, et al. Post COVID-19 syndrome with impairment of flow-mediated epicardial vasodilation and flow reserve. *Eur J Clin Invest*. 2022;00:e13871. doi: [10.1111/eci.13871](https://doi.org/10.1111/eci.13871)